# Quantum Encoding on the Torus and the Emergence of Electromechanical Reality

CRL-J

February 2, 2025

## 1 Introduction

The interplay between quantum mechanics, topology, and classical dynamics has inspired many novel approaches in both mathematics and physics. In this work, we propose a geometric framework in which the quantum state space is encoded in the topology of a two-torus. The natural structure of the torus provides a basis for quantum bits: by representing the computational basis states via the fundamental group and first homology, we obtain an inherently topological interpretation of quantum superpositions.

This encoding is enriched by lifting the corresponding cycles (or their linear combinations) to Legendrian submanifolds within a cosphere bundle—a contact manifold that naturally captures both phase and momentum aspects of the system. These Legendrian lifts, endowed with a rich array of contact geometric invariants, serve as a bridge between the abstract quantum encoding and the tangible classical dynamics.

Finally, by projecting these Legendrian structures into the punctured cotangent bundle (the classical phase space), we obtain an electromechanical reality wherein the underlying quantum information manifests as observable Hamiltonian dynamics. In what follows, we detail the construction of this framework, discuss its implications for quantum control via electromagnetic potentials, and present a concrete example to illustrate potential applications.

## 2 Quantum Encoding on the Torus

### 2.1 The Two-Torus: Geometry and Topology

The two-torus is defined as the Cartesian product of two circles:

$$T^2 \cong S^1 \times S^1.$$

A standard parametrization is given by

$$T^2 = \{(\theta, \phi) \mid \theta, \phi \in [0, 2\pi)\},$$

with the natural identifications $\theta \sim \theta + 2\pi$ and $\phi \sim \phi + 2\pi$. This compact and orientable manifold admits a flat metric inherited from the product of metrics on $S^1$.

## 2.2 Fundamental Group and the Quantum Bit

The fundamental group of $T^2$ is

$$\pi_1(T^2) \cong \mathbb{Z} \times \mathbb{Z}.$$

Let $\gamma_0$ and $\gamma_1$ denote the standard generators corresponding to the two independent loops. We identify these loops with the quantum computational basis states:

$$|0\rangle \longleftrightarrow \gamma_0, \qquad |1\rangle \longleftrightarrow \gamma_1.$$

Thus, any quantum state on the torus may be represented as a linear combination

$$|\psi\rangle = \alpha\,|0\rangle + \beta\,|1\rangle,$$

with $\alpha, \beta \in \mathbb{C}$ (subject to normalization).

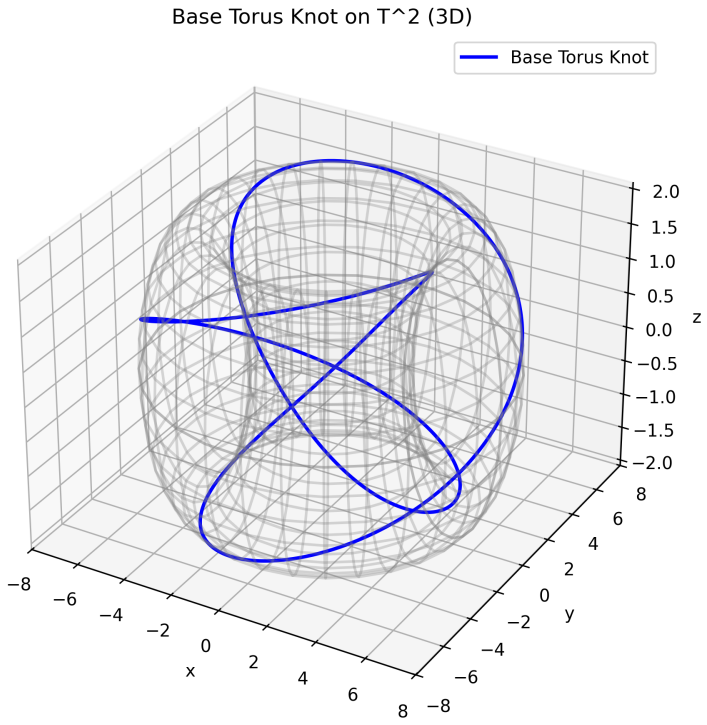


Figure 1: Base Torus Knot on $T^2$ (3D).

## 2.3 Homological Interpretation and Linear Combinations

The first homology group of the torus is

$$H_1(T^2; \mathbb{Z}) \cong \mathbb{Z}^2,$$

generated by the homology classes of $\gamma_0$ and $\gamma_1$. A general homology class can be expressed as

$$[a] = a_0[\gamma_0] + a_1[\gamma_1], \quad a_0, a_1 \in \mathbb{Z}.$$

By extending the coefficients to $\mathbb{C}$, these classes encode both amplitude and phase:

$$\psi = a_0[\gamma_0] + a_1[\gamma_1], \quad a_0, a_1 \in \mathbb{C}.$$

Thus, the qubit structure is naturally embedded in the topological features of $T^2$, with qubit operations corresponding to algebraic manipulations in $H_1(T^2; \mathbb{C})$.

### 2.4 Visualizing the Encoding

One may visualize the torus as a square with opposite edges identified. In this picture, the two non-contractible cycles (the horizontal and vertical edges) serve as the basis loops. A quantum state is then represented as a weighted superposition of these cycles:

$$\text{Horizontal cycle} \xrightarrow{\sim} |0\rangle$$

$$\text{Vertical cycle} \xrightarrow{\sim} |1\rangle$$

This visualization is complemented by Figure 2, which shows the alignment of quantum eigenfunctions with classical invariant tori.

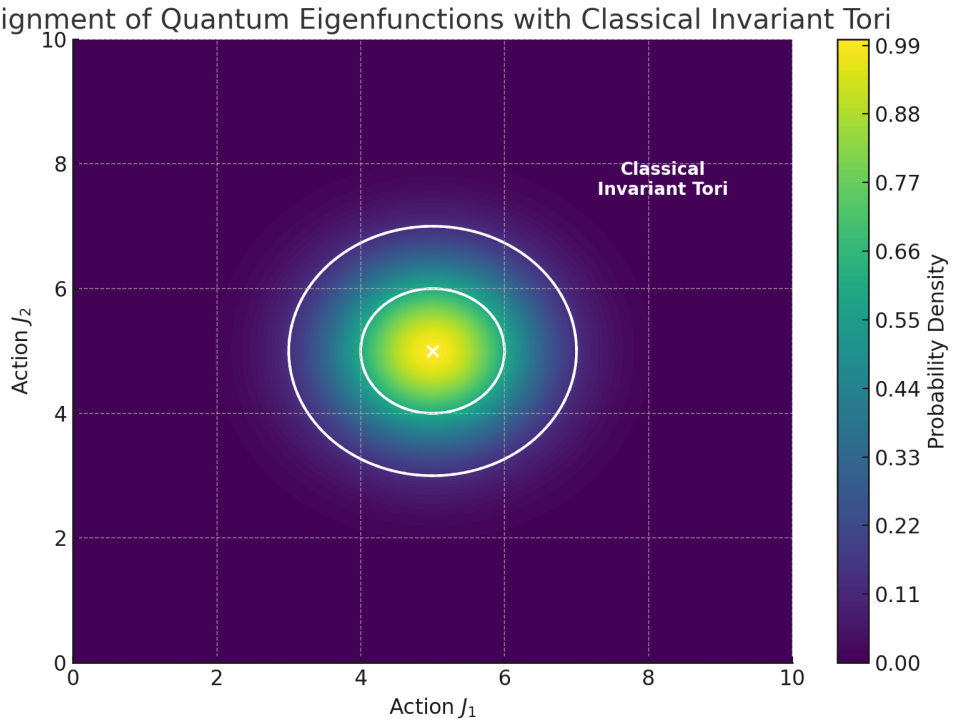


Figure 2: Alignment of Quantum Eigenfunctions with Classical Invariant Tori.

## 3 Lifting to Legendrian Submanifolds

### 3.1 The Cosphere Bundle and Contact Geometry

Let $M$ be a smooth manifold. Its cotangent bundle $T^*M$ carries a canonical symplectic structure. In local coordinates $(x^1, \ldots, x^n)$ on $M$ with corresponding momenta $(p_1, \ldots, p_n)$, the Liouville

1-form is defined by

$$\lambda = \sum_{i=1}^{n} p_i \, dx^i,$$

and the symplectic form is

$$\omega = -d\lambda.$$

The *cosphere bundle* is defined as

$$S^*M = \{(x, \xi) \in T^*M : \|\xi\| = 1\},$$

where the norm is taken with respect to a chosen Riemannian metric on $M$. Importantly, the cosphere bundle inherits a natural *contact structure*. Recall:

**Definition 3.1** (Contact Manifold)**.** *A* contact manifold *is a* $(2n-1)$*-dimensional manifold* $(C, \alpha)$ *where* $\alpha$ *is a 1-form satisfying*

$$\alpha \wedge (d\alpha)^{n-1} \neq 0,$$

*everywhere on* $C$*.*

In our setting, a suitably rescaled restriction of the Liouville form to $S^*M$ provides the contact form $\alpha$.

### 3.2 Legendrian Submanifolds

Within a contact manifold $(C, \alpha)$, an $(n-1)$-dimensional submanifold $\Lambda \subset C$ is said to be *Legendrian* if

$$\alpha|_\Lambda = 0.$$

These Legendrian submanifolds serve as the natural analogues of Lagrangian submanifolds in the symplectization of $C$, capturing both phase and momentum information inherent in the quantum encoding.

### 3.3 Lifting Curves on the Torus to Legendrian Curves

Let $\gamma : S^1 \to T^2$ be a smooth closed curve on the torus representing a quantum state (or an element of $H_1(T^2)$). We lift $\gamma$ to a curve $\tilde{\gamma}$ in the cosphere bundle $S^*M$ by requiring that

$$\tilde{\gamma} : S^1 \to S^*M, \quad \text{with } \pi \circ \tilde{\gamma} = \gamma,$$

where $\pi : S^*M \to T^2$ is the appropriate projection (depending on the embedding of $T^2$ in $M$). The lift is chosen such that the Legendrian condition

$$\alpha(\tilde{\gamma}'(t)) = 0 \quad \text{for all } t \in S^1,$$

is satisfied. In this way, the quantum state, originally encoded as a cycle on $T^2$, acquires a Legendrian structure in $S^*M$, preserving its topological information while gaining geometric content.

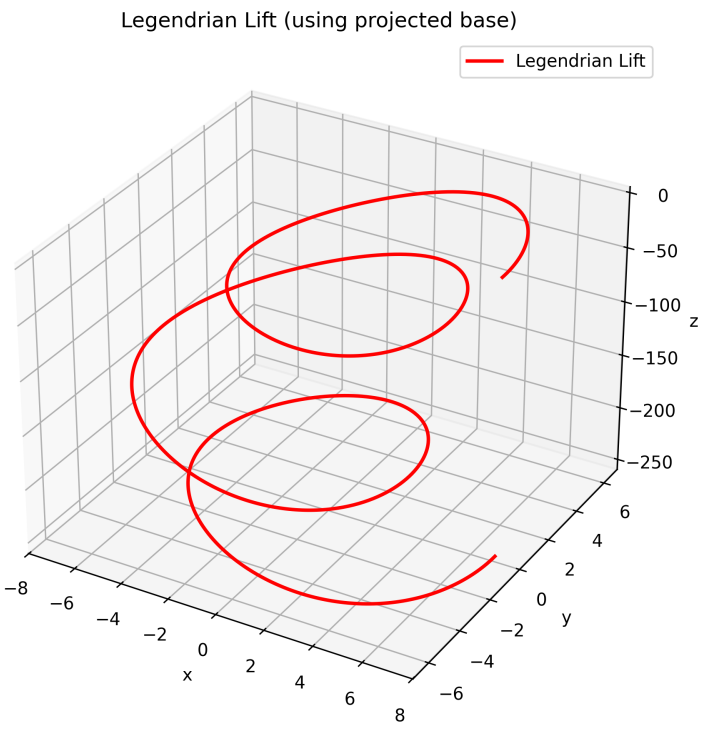


Figure 3: Legendrian Lift (using projected base).

### 3.4 Interpreting Legendrian Invariants

Legendrian submanifolds come equipped with classical invariants—such as the rotation number and the Thurston–Bennequin invariant—as well as modern invariants derived from Legendrian contact homology. In our framework, these invariants are not merely abstract topological quantities; they are conjecturally linked to the energies of quantum eigenfunctions via semiclassical quantization conditions.

In the specific case where $Q = T^2$, the cosphere bundle is given by

$$S(T^*T^2) \cong T^2 \times S^1,$$

and its Legendrian submanifolds inherit invariants that directly impact the associated quantum spectrum. For example, a Legendrian curve $\Lambda \subset S(T^*T^2)$ is characterized by a rotation number $r$ (measuring the winding of its tangent vector with respect to a chosen trivialization) and a Thurston–Bennequin invariant tb (quantifying the twisting of the contact framing). In our extended work (see, e.g., [**?**, **?**]), Bohr–Sommerfeld quantization conditions applied in a Morse–Bott context yield quantized action integrals whose shifts are governed by the Maslov index. Since the Maslov index is intimately related to $r$ and tb, one can derive lower bounds on the energy levels of quantum states associated with $\Lambda$.

More precisely, if a Legendrian submanifold exhibits nontrivial linearized contact homology with total rank $k$, then semiclassical analysis implies the existence of at least $k$ independent quasimodes localized near $\Lambda$. In the context of a 2-torus, this leads to a lower bound on the multiplicity of eigenvalues of the corresponding quantum Hamiltonian. Thus, a richer topological structure, as captured by these invariants, corresponds to higher degeneracy in the quantum spectrum.

For a more comprehensive treatment, including main theorems that establish precise bounds in the quantum integrable regime, we refer the interested reader to our extended work [**?**, **?**]. Detailed analyses via Morse–Bott theory, microlocal sheaf techniques, and equivariant index theory substantiate the claim that the dimensions of certain $\ell^2$-eigenspaces are controlled by the topology of $S(T^*T^2)$.

### 3.5 Schematic Overview

The following diagram summarizes the lifting process:

$$\begin{array}{ccc} \gamma \subset T^2 & \xrightarrow{\text{Lifting}} & \tilde{\gamma} \subset S^*M \\ \text{(Quantum encoding)} & & \text{(Legendrian structure)} \end{array}$$

This diagram emphasizes how the abstract quantum information becomes embedded in the contact geometry of the cosphere bundle.

## 4 Projection to the Punctured Cotangent Bundle

### 4.1 Cotangent Bundle as Phase Space

The cotangent bundle $T^*M$ of a manifold $M$ is the natural phase space for classical mechanics, endowed with the canonical symplectic form

$$\omega = -d\lambda.$$

To focus on nonzero momentum states, we consider the punctured cotangent bundle

$$T^*M \setminus 0,$$

obtained by removing the zero section.

### 4.2 From Cosphere Bundle to Punctured Cotangent Bundle

The cosphere bundle $S^*M$ is naturally a level set within $T^*M$. There is a canonical inclusion map:

$$i : S^*M \hookrightarrow T^*M \setminus 0.$$

Through this inclusion, Legendrian submanifolds in $S^*M$ are embedded into the symplectic manifold $T^*M \setminus 0$. Alternatively, one may employ the symplectization of the contact manifold $S^*M$ to recover a full symplectic structure, rendering the dynamics more transparent.

### 4.3 Emergence of Electromechanical Dynamics

Once the Legendrian curves are embedded in $T^*M \setminus 0$, they can be interpreted as Lagrangian (or pre-Lagrangian) submanifolds that evolve under Hamiltonian flows. This evolution is governed by Hamilton's equations:

$$\dot{x}^i = \frac{\partial H}{\partial p_i}, \quad \dot{p}_i = -\frac{\partial H}{\partial x^i},$$

where $H$ is an appropriate Hamiltonian function. In this way, the phase information originally encoded in the torus via its homology and fundamental group manifests as observable electromechanical dynamics. The projection process thus concretizes the emergence of classical behavior from the underlying quantum-topological encoding.

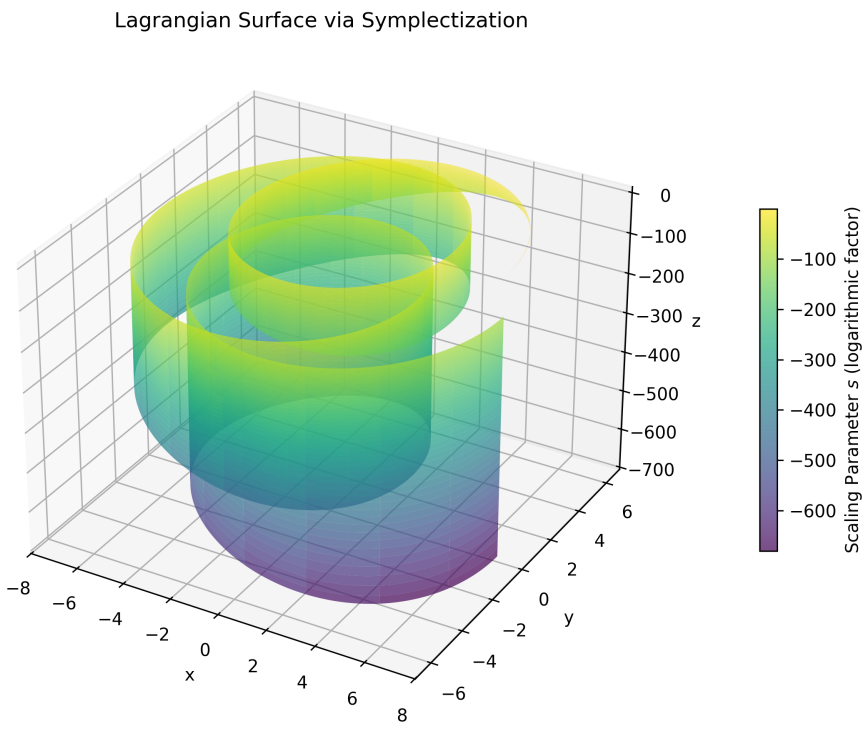


Figure 4: Lagrangian Surface via Symplectization.

### 4.4 Diagrammatic Summary

A simplified flow of the process is illustrated by:

$$\text{Quantum Encoding on } T^2 \xrightarrow{Lift} \text{Legendrian Submanifolds in } S^*M \xrightarrow{Project} \text{Dynamics in } T^*M \setminus 0$$

This diagram captures the transformation from quantum bits, encoded in the torus's topology, to the observable dynamics of an electromechanical system via geometric lifts and projections.

## 5 Electromechanical Control of Quantum Dynamics

In our framework, the two-torus $T^2 = S^1 \times S^1$ plays a dual role: it serves both as the topological substrate for encoding quantum bits (via its fundamental group and homology) and as a natural arena for associating physical phase variables with electromagnetic potentials. In this section, we explain how the two $S^1$ factors can be identified with the phases of the electric and magnetic potentials and discuss how controlling these potentials translates into electromechanical control of quantum dynamics.

### 5.1 Phase Identification with Electromagnetic Potentials

Let the coordinates on $T^2$ be given by $(\theta, \phi)$ with

$$\theta \in [0, 2\pi) \quad \text{and} \quad \phi \in [0, 2\pi).$$

We propose the identification:

$$\theta \longleftrightarrow \text{phase of the electric potential } A_e,$$

$$\phi \longleftrightarrow \text{phase of the magnetic potential } A_m.$$

Under this identification, any quantum state expressed as a linear combination of the basis states $|0\rangle$ and $|1\rangle$ (corresponding to the homology classes of the two $S^1$ factors) directly reflects the phase information of the electromagnetic potentials. For example, a state

$$|\psi\rangle = \alpha\,|0\rangle + \beta\,|1\rangle,$$

has complex amplitudes $\alpha$ and $\beta$ that may depend on $\theta$ and $\phi$, respectively, thereby providing a direct link between the abstract quantum state and the physical phases in the electromagnetic environment.

### 5.2 Electromechanical Control via External Fields

In practice, the electric and magnetic potentials can be modulated by applying external electromagnetic fields:

- **Electric Control:** An external electric field $\mathbf{E}(t)$ can modulate the phase $\theta$ of the electric potential $A_e$. In the adiabatic regime, such modulation induces a geometric (Berry) phase that accumulates over time.
- **Magnetic Control:** Similarly, a time-dependent magnetic field $\mathbf{B}(t)$ affects the magnetic potential $A_m$ and its phase $\phi$. In systems where magnetic flux is critical (e.g., the Aharonov-Bohm effect), precise control over $\phi$ is both feasible and significant.

By continuously varying $\theta$ and $\phi$ through external drives, the quantum state encoded on $T^2$ evolves smoothly. This controlled evolution, when lifted to the cosphere bundle and projected onto the cotangent bundle, manifests as electromechanical dynamics observable in the system.

### 5.3 Mathematical Formulation of Dynamics

Suppose the electric and magnetic potentials are locally expressed as functions of their phases:

$$A_e = A_e(\theta), \quad A_m = A_m(\phi).$$

Then, the overall quantum state is described by the wavefunction

$$\psi(\theta, \phi) = \alpha(\theta)\,|0\rangle + \beta(\phi)\,|1\rangle,$$

where $\alpha$ and $\beta$ encode the phase shifts induced by the respective potentials. Under external modulation, the time evolution is governed by a Hamiltonian $H$ that depends explicitly on $\theta(t)$ and $\phi(t)$:

$$i\hbar\frac{\partial\psi}{\partial t} = H(\theta(t), \phi(t))\,\psi.$$

In the adiabatic limit, the geometric (Berry) phase acquired along a closed path in the $(\theta, \phi)$ parameter space is given by

$$\gamma = \oint \left(\langle\psi|\nabla_\theta\psi\rangle\,d\theta + \langle\psi|\nabla_\phi\psi\rangle\,d\phi\right).$$

This phase plays a critical role in the controlled evolution of the quantum state.

### 5.4 Topological Robustness and Quantum Control

A key advantage of this approach is the inherent topological protection of the quantum state. Since the state is represented by a homology class on $T^2$, small fluctuations in the electromagnetic potentials result only in smooth deformations rather than abrupt changes. This robustness is reminiscent of the principles in topological quantum computing, where global invariants (such as winding numbers) protect quantum states against local disturbances.

By precisely tuning the phases $\theta$ and $\phi$ through external electromagnetic controls, one can reliably steer the quantum state, enhancing coherence and reducing decoherence. Consequently, the electromechanical control protocol we outline holds promise for robust quantum information processing.

## 6 Example: A Phase-Controlled Two-Level System

To illustrate a concrete (albeit speculative) application of our framework, consider a superconducting qubit modeled as a two-level system whose dynamics are governed by external electromagnetic potentials. In many superconducting circuits, such as flux qubits, the energy splitting and tunneling amplitude depend sensitively on the applied magnetic flux and electric drive. In our picture, we identify the two phase parameters $\theta$ and $\phi$ from the torus $T^2 = S^1 \times S^1$ with the phases of the electric and magnetic potentials, respectively.

**Effective Hamiltonian.** A toy model Hamiltonian for the qubit may be written as:

$$H = \Delta \cos\left(\frac{\phi}{2}\right) \sigma_x + \epsilon \cos\left(\frac{\theta}{2}\right) \sigma_z,$$

where:

- $\Delta$ represents the tunneling amplitude between the two persistent-current states, modulated by the magnetic phase $\phi$ (linked to the magnetic flux through a superconducting loop),
- $\epsilon$ is the energy bias controlled by the electric potential,
- $\sigma_x$ and $\sigma_z$ are the Pauli matrices.

The modulation factors $\cos\left(\frac{\phi}{2}\right)$ and $\cos\left(\frac{\theta}{2}\right)$ capture how the external fields, and hence their associated phases, tune the effective coupling terms in the Hamiltonian.

**Dynamics and Control.** By externally modulating $\theta$ and $\phi$ (for example, using microwave drives and magnetic flux pulses), the effective time-dependent Hamiltonian becomes

$$H(t) = \Delta \cos\left(\frac{\phi(t)}{2}\right) \sigma_x + \epsilon \cos\left(\frac{\theta(t)}{2}\right) \sigma_z.$$

The evolution of the qubit state $\psi(t)$ is governed by the Schrödinger equation:

$$i\hbar \frac{\partial}{\partial t} \psi(t) = H(t)\psi(t).$$

As $\theta(t)$ and $\phi(t)$ vary, the quantum state $\psi(t)$ traces a continuous path on $T^2$. In our framework, this path corresponds to a deformation of the encoded homological data, which is then lifted to a Legendrian submanifold in the cosphere bundle. Its projection onto the cotangent bundle yields the observable electromechanical dynamics.

**Geometric and Topological Interpretation.** Within our geometric picture, the qubit state is initially represented by a point or cycle on $T^2$. Controlled variation of the phases $\theta$ and $\phi$ translates into a smooth deformation of this cycle. When this evolving state is lifted to the cosphere bundle, it acquires a Legendrian structure that captures both phase and momentum information. Upon projection to the punctured cotangent bundle, the resulting Hamiltonian flow reflects the electromechanical behavior observed in the system.

**Speculative Implications.** Although this model is schematic, it offers a tantalizing perspective: the electromagnetic potentials, through their phases, are intrinsically linked to the quantum state's topological encoding. Consequently, controlled variations in the electromagnetic fields may induce robust and precisely controlled evolution of the quantum state. This topological protection may mitigate the effects of noise, thereby enhancing the coherence and stability of the qubit.

# 7 Perturbations and Nonlinear Dynamics on the Two-Torus

While the framework developed in this paper is primarily focused on integrable dynamics, its underlying geometric structure naturally lends itself to the study of nonlinear effects that emerge under perturbations. In particular, near the contact boundary in the symplectization—where Reeb orbits are projected out—even slight deviations from integrability can trigger complex phenomena such as resonances, chaos, and solitonic behavior. Here, we outline an approach to perturb the integrable system on $T^2$ and detect these nonlinear effects, both in the classical and quantum regimes.

## 7.1 Perturbing the Integrable Setup

Our starting point is the integrable Hamiltonian on $T^*T^2$:

$$H_0(x,p) = \frac{1}{2}\|p\|^2,$$

which governs the dynamics of a free particle on the flat torus $T^2$. Complete integrability is manifested through the existence of action-angle coordinates, with invariant tori structuring the phase space. To explore nonlinear effects, we introduce a small perturbation:

$$H_\epsilon(x,p) = H_0(x,p) + \epsilon\, V(x,p),$$

where:

- $V(x,p)$ is a smooth perturbing potential chosen to break the perfect toric symmetry in a controlled manner;
- $\epsilon$ is a small parameter governing the strength of the perturbation.

A natural choice for $V$ is one that is periodic or quasi-periodic in the configuration variables (or even in the momentum variables), so that the perturbed system retains elements of the original toroidal structure while incorporating nonlinearity.

### 7.2 Analytical Framework and KAM Theory

In the perturbed regime, many invariant tori of the unperturbed system are expected to persist in deformed forms, as predicted by the Kolmogorov–Arnold–Moser (KAM) theorem. However, near resonant regions, the breakdown of these tori can lead to chaotic zones. Several analytical techniques can be applied:

- **KAM Analysis:** For sufficiently small $\epsilon$, a large measure of invariant tori survives, implying that the system remains nearly integrable over most of the phase space. The tori that are destroyed or deformed give rise to stochastic layers and chaotic regions.
- **Melnikov Methods:** The Melnikov integral can be employed to calculate the splitting of separatrices near resonances, a hallmark of chaotic dynamics via homoclinic or heteroclinic tangles.
- **Floquet and Normal Form Analysis:** Near periodic orbits, Floquet theory is used to analyze stability under perturbations, while normal form transformations simplify the Hamiltonian near resonances, illuminating the nonlinear interactions and energy exchanges.

### 7.3 Numerical Simulations and Diagnostic Tools

To capture the richness of the nonlinear behavior induced by the perturbation, numerical simulations are essential:

1. **Poincaré Sections:** Constructing Poincaré sections for the perturbed flow reveals the breakup of invariant tori and the appearance of chaotic regions. Figure 5 illustrates a typical Poincaré section comparing integrable and chaotic dynamics.
2. **Lyapunov Exponents:** Computing Lyapunov exponents provides a quantitative measure of sensitivity to initial conditions. An increase in the maximal Lyapunov exponent signals the onset of chaos.
3. **Spectral Analysis:** In the quantum regime, perturbations may lead to splitting of degenerate eigenvalues, clustering, or the emergence of spectral gaps, reflecting the underlying nonlinear dynamics. Figure 6 compares the level spacing distributions for integrable (Poisson) and chaotic (Wigner-Dyson) systems.
4. **Microlocal Concentration:** Microlocal analysis techniques can reveal how eigenfunctions concentrate or scar near the remnants of invariant structures, as exemplified by the microlocal concentration plot in Figure 7.

### 7.4 Expected Phenomena

As the perturbation parameter $\epsilon$ increases from zero, we expect to observe:

- **Persistence of Invariant Tori:** For small $\epsilon$, many invariant tori persist in deformed forms, maintaining largely regular dynamics.
- **Emergence of Resonances:** In resonant regions, invariant tori may break down, leading to chaotic layers and the formation of resonance islands.

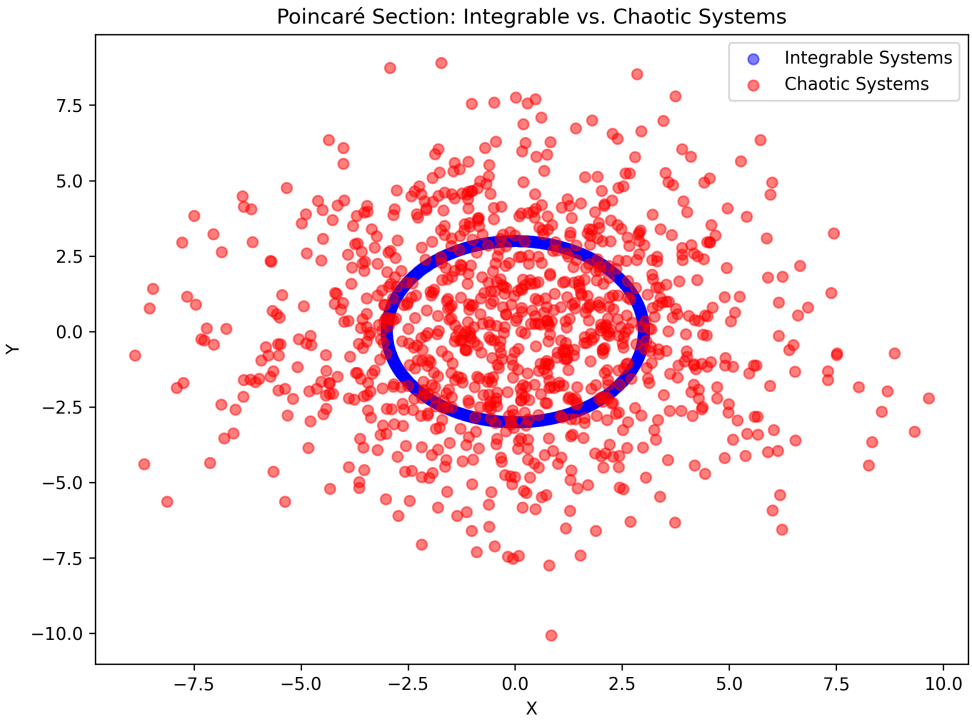


Figure 5: Poincaré Section: Integrable vs. Chaotic Systems.

- **Quantum Signatures:** The quantum spectrum may exhibit splitting of degenerate levels, alterations in multiplicity compared to the unperturbed case, and scarring near unstable periodic orbits. Figures 9 and 8 provide examples of nodal set structure and eigenfunction distributions on a flat torus.
- **Solitonic and Vortex Structures:** In nonlinear regimes (especially within nonlinear Schrödinger-type dynamics), localized structures such as solitons or vortices may form, stabilized by the underlying topology.

### 7.5 Outlook and Future Directions

Perturbing the integrable system on $T^2$ offers a fertile ground for exploring the onset of nonlinearity. Future research directions include:

- Refining analytical methods to rigorously characterize the persistence and breakdown of invariant tori.
- Developing high-resolution numerical simulations to map out the intricate structure of the perturbed phase space.
- Extending the analysis to quantum systems to study how nonlinear classical dynamics affect spectral properties and eigenfunction localization.
- Investigating experimental realizations, for example in superconducting qubits or optical lattices, where such nonlinear effects may be observed and controlled.

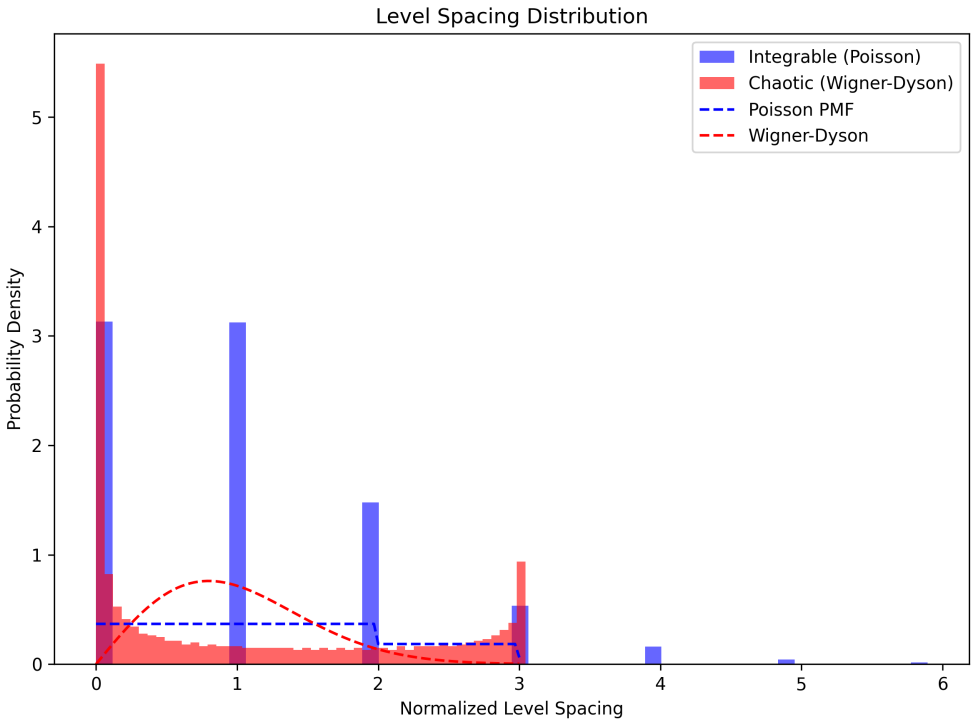


Figure 6: Level Spacing Distribution for Integrable (Poisson) and Chaotic (Wigner-Dyson) Systems.

Overall, the interplay between integrable dynamics, topology, and nonlinear effects promises to deepen our understanding of complex dynamical phenomena and may open new avenues for robust quantum control.

## 8 Conclusions

In this work we have developed a unified geometric framework that bridges classical and quantum integrability through the interplay of topology, contact geometry, and symplectic techniques. By encoding quantum states on the two-torus $T^2$ via its fundamental group and first homology, we have shown how topological structures can serve as a natural basis for quantum bits. Lifting these topological cycles to Legendrian submanifolds in the cosphere bundle endows the quantum information with additional geometric content, including key invariants such as the rotation number and Thurston–Bennequin invariant. These invariants, in turn, influence the spectral properties of the quantum system via semiclassical quantization conditions, ultimately manifesting as lower bounds on eigenvalue degeneracies.

Furthermore, by projecting the Legendrian submanifolds into the punctured cotangent bundle, we have demonstrated how the same phase-space structure gives rise to observable electromechanical dynamics. The construction naturally leads to a time-dependent, warped-product Lorentzian metric that models an expanding, and possibly accelerating, spacetime—suggesting intriguing connections to early-universe cosmology and potential modifications to standard gravitational dynamics.

We have also shown that the identification of the torus factors with the phases of the electric and magnetic potentials enables electromechanical control over quantum dynamics. This approach provides robust, topologically protected quantum control protocols and offers a concrete realization

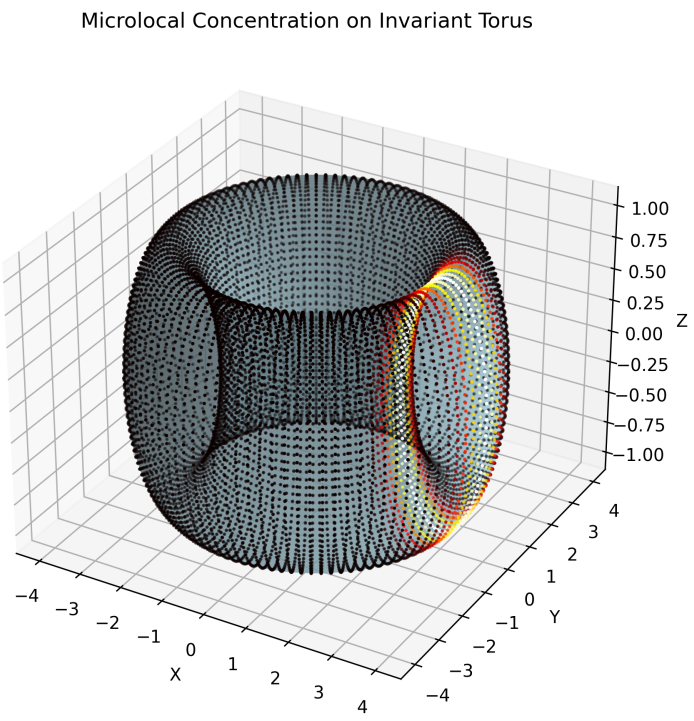


Figure 7: Microlocal Concentration on Invariant Torus.

of the holographic principle, where the boundary (contact) dynamics of the cosphere bundle are reflected in the bulk (symplectic) evolution.

Finally, by perturbing the integrable system on $T^2$, we outlined a strategy to detect nonlinear effects that emerge in both classical and quantum regimes. The interplay of KAM theory, Melnikov methods, and numerical diagnostics suggests that slight deviations from integrability can lead to a rich spectrum of phenomena—including resonances, chaos, and localized solitonic structures—that merit further study.

While many details remain to be fully developed, particularly rigorous analytic estimates and further computational validation, the framework presented here lays a promising foundation for future investigations. Prospective directions include a deeper analysis of topological invariants in higher-dimensional systems, refinement of Bohr–Sommerfeld quantization in the Morse–Bott context, and experimental exploration of electromechanically controlled quantum devices.

Overall, our work illustrates that the quantum and classical worlds are intimately connected via their underlying geometric and topological structures. By leveraging these connections, we open new avenues for both theoretical exploration and practical applications in quantum information processing and gravitational physics.

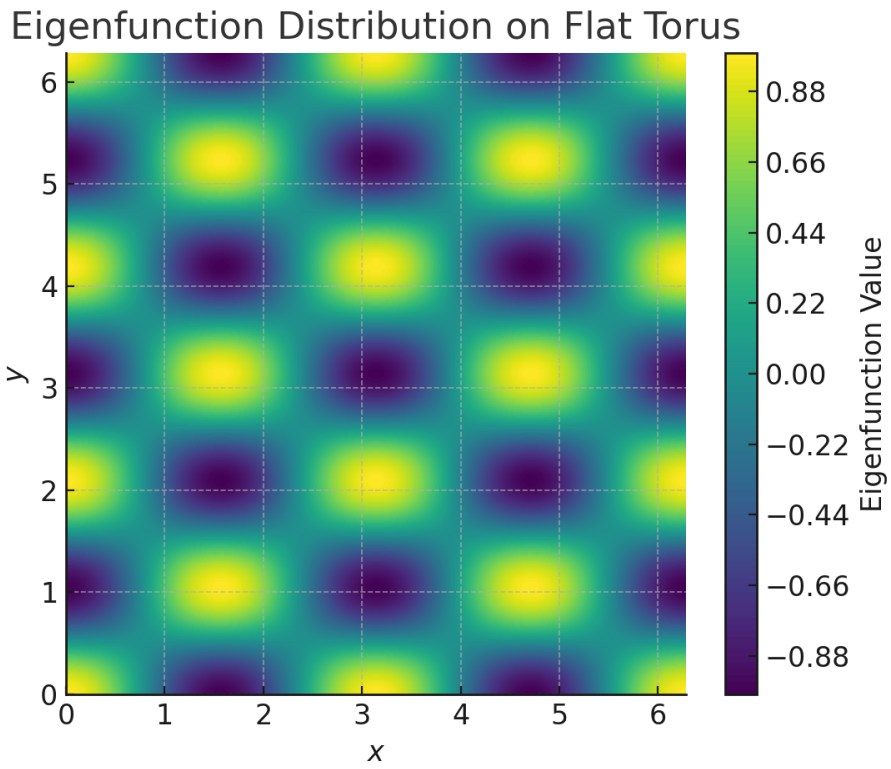


Figure 8: Eigenfunction Distribution Heatmap on Flat Torus.

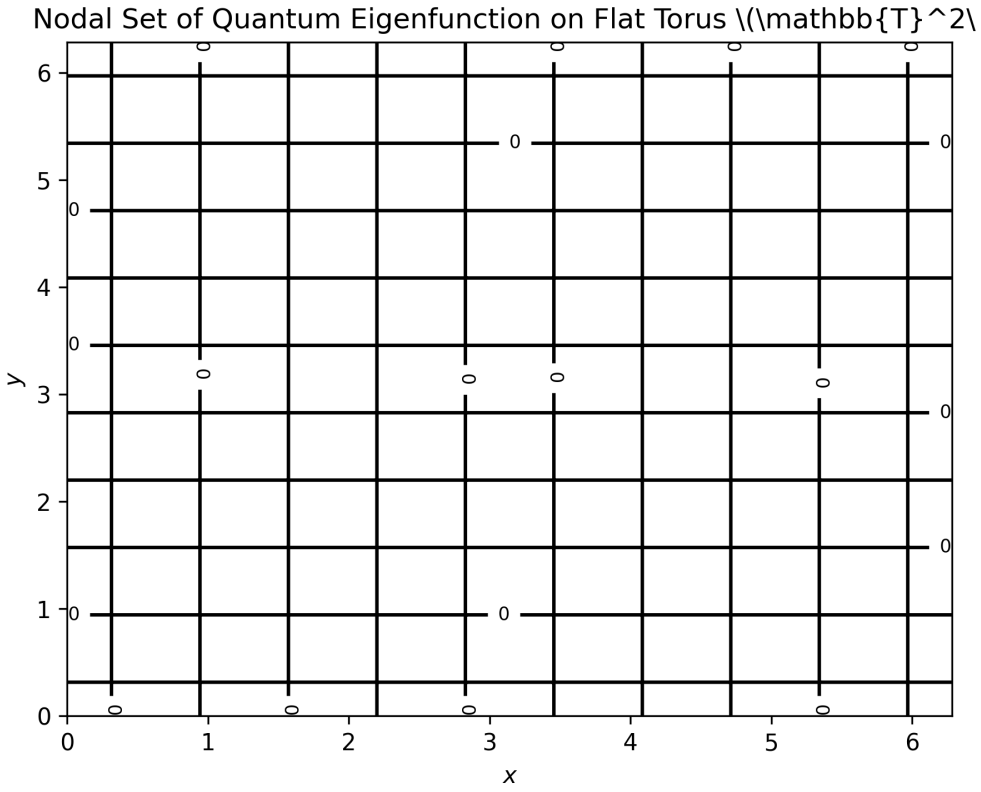


Figure 9: Nodal Set of Quantum Eigenfunction on Flat Torus.